Available online at www.sciencedirect.com

Food and Bioproducts Processing

journal homepage: www.elsevier.com/locate/fbp

A simple process to purify (*E*)-resveratrol from grape stems with a photo-molecularly imprinted sorbent

A. Bzainia[a,b], R.C.S. Dias[a,*], M.R.P.F.N. Costa[b]

[a] Polytechnic Institute of Bragança-Mountain Research Center (CIMO), Bragança 5300-253, Portugal
[b] LSRE-LCM-Laboratory of Separation and Reaction Engineering—Laboratory of Catalysis and Materials, Faculty of Engineering, Department of Chemical Engineering, University of Porto, Porto 4200-465, Portugal

ARTICLE INFO

Article history:
Received 17 May 2023
Received in revised form 22 August 2023
Accepted 24 August 2023
Available online 28 August 2023

Keywords:
Photo-molecularly imprinted sorbent
(*E*)-resveratrol purification
Sorption-desorption processes
Winemaking residues
Circular bioeconomy

ABSTRACT

The present work focused on the development of a process of sorption-desorption to purify (*E*)-resveratrol found in winemaking residues, specifically from the crude extract of grape stems. The core element of this process is a photo-molecularly imprinted sorbent (MIS) synthesized by means of the molecular imprinting technique (MIT). This sorbent is a 4-vinylpyridine rich polymer network which binds (*E*)-resveratrol at stereospecific sites. Comparison of sorption isotherms of the MIS and its counterpart non-imprinted sorbent (NIS) shows the higher capability of the MIS to bind (*E*)-resveratrol. It is noteworthy that the size of MIS particles was larger than to those of the NIS (as found by scanning electron microscopy analysis) facilitating its use in sorption-desorption processes without reaching a high backpressure. The MIS was then used to purify (*E*)-resveratrol from grape stems extract in a two-step purification procedure through a simple device. The initial purification step permitted to increase the purity of (*E*)-resveratrol from 29% to 78% (34% of recovery), whereas a further one took it to 87% (70% of recovery). The purified fractions were obtained in hydroalcoholic medium and contained other bioactive stilbenes such as (*E*)-ε-viniferin. The results of this research provide a compelling proof of concept for room-temperature photopolymerization, enabling the development of highly efficient imprinted polymers as sorbents for purifying bioactive compounds from agricultural residues. This significant advancement paves the way for its large-scale implementation in a circular bioeconomy approach.

1. Introduction

Winemaking residues contain a diverse array of phenolic compounds ranging from flavonoids, phenolic acids, stilbenes and even macromolecules such as tannins (Acquadro et al., 2020; Tapia-Quirós et al., 2022). Among this plethora of polyphenols, (*E*)-resveratrol is of particular interest due to its inherent antioxidant and anti-inflammatory activities. As a matter of fact, (*E*)-resveratrol has been reported to be cardioprotective (Chopra et al., 2022), to confer neuroprotection against Alzheimer's disease (Islam et al., 2022) and to improve energy utilization when performing short-duration high-intensity exercises (Su et al., 2023). The occurrence of stilbenes and especially (*E*)-resveratrol in grape stems has

* Corresponding author.
E-mail address: rdias@ipb.pt (R.C.S. Dias).
https://doi.org/10.1016/j.fbp.2023.08.010

been put into evidence by several previous works (Ji et al., 2014; Fabjanowicz et al., 2018; Esparza et al., 2021; Bzainia et al., 2023).

In fact, grape stems are generally removed from bunches prior to fermentation, and they can represent up to 6–7% of the weight of grapes. Often, grape stems are applied to the soil as organic and mineral inputs although with low efficacy due to its low biodegradability. Previous studies demonstrated that this biomass is a source of sugars and interesting bio-compounds, namely resveratrol, with applications in the food and other industries (del et al., 2022). It is reported that one ton of processed grapes (global annual production ~8 $\times 10^7$ tons) generates about 30–40 kg of grape stems (del et al., 2022) and therefore around 2.8 $\times$ 10^6 tons of this biomass are potentially available as a proper feedstock for the valorization of (*E*)-resveratrol.

In this context, having a selective sorbent able to retain (*E*)-resveratrol from the crude extract of grape stems would avoid the recourse to several treatment steps which are often needed to isolate this bioactive compound due to its chemical similarity to other stilbenes.

A bibliographic review allowed to scout the main techniques that have been used to valorize (*E*)-resveratrol from various matrices. Most purification procedures focus on the use of commercial sorbents (Wang et al., 2021; Jia et al., 2020; Zhang et al., 2009; Xiong et al., 2014; Sun et al., 2018) which are not specific to the molecule of (*E*)-resveratrol. This naturally leads to the employment of various techniques during the purification process of (*E*)-resveratrol to compensate for the commercial sorbent's lack of specificity (Zhang et al., 2009; Liu et al., 2021). Obviously, this hinders the scale-up of the purification process from an economical point of view.

In the present work, we tackled this issue through the use of a tailor-made sorbent in a continuous process of sorption-desorption to valorize (*E*)-resveratrol from grape stems extract. This sorbent was synthesized using the molecularly imprinting technique (MIT) in combination with photo-polymerization leading to the creation of three-dimensional cavities specific to (*E*)-resveratrol. Although previous studies have reported the synthesis of molecularly imprinted sorbents for the retention of (*E*)-resveratrol (Schwarz et al., 2011a; Cao et al., 2021), few of them have demonstrated its applicability to treat complex extracts where the selective retention of (*E*)-resveratrol is not straightforward (Cao et al., 2021; Schwarz et al., 2011b).

The photo-molecularly imprinted sorbent (MIS) used to purify (*E*)-resveratrol from grape stems extract, was synthesized in the framework of our recently published work (Bzainia et al., 2023) where a systematic synthesis based on factorial design was carried out allowing to obtain different MISs and their correspondent non-imprinted sorbents (NISs). The synthesized materials were based on the functional monomer 4-vinylpyridine (4VP) and were polymerized through UV irradiation at ambient room temperature using (*E*)-resveratrol as the imprinting molecule. The use of room temperature photo-polymerization was a step towards the greenification (Arabi et al., 2021) of the process and avoided the disruption of the intermolecular interactions between 4VP and (*E*)-resveratrol. In fact, it is of common knowledge that intermolecular forces do severely weaken as heat is applied to the polymerization environment resulting in a loss of specificity of the MIS towards the target compound (Mizan et al., 1996; Cormack and Elorza, 2004). The synthesized sorbents were subject to sorption tests from which it was put into evidence the clear advantage of the MISs in comparison to the NISs, thus showcasing the relevance of the MIT to modify the recognition capabilities of the sorbents (Bzainia et al., 2023). Eventually, among the different synthesized materials, one specific MIS was chosen (referred to as MIP7 in our previous work (Bzainia et al., 2023)) due to its dual imprinting factor and binding capacity for (*E*)-resveratrol. This MIS played the role of the core element of the purification process proposed herein. This latter does not require any form of extract pre-treatment or the use of different purification techniques. It mainly relies on the sorption of the extract followed by desorption using selected solvents.

This current study builds upon the findings of our previous one (Bzainia et al., 2023) where the suitable polymerization conditions of the functional MIS were fixed. And to the best of our knowledge, the use of a photo-molecularly imprinted sorbent to target (*E*)-resveratrol present in the grape stems has not been reported.

2. Materials and methods

2.1. Reagents

All chemicals were used as purchased, without further purification. The standard of (*E*)-resveratrol (≥ 98%) was purchased from Cayman (USA). The monomer 4-vinylpyridine (4VP, ≥ 95%) was purchased from Alfa Aesar (USA). The styrene monomer (STY, ≥ 99%) and the crosslinker ethylene glycol dimethacrylate (EGDMA, ≥ 98%) were acquired from Sigma Aldrich (Germany). The polymerization initiator 2,2′-azobis(2-methylpropionitrile) (AIBN, ≥ 98%) was purchased from Sigma Aldrich (Germany). The solvent dimethylformamide (DMF, ≥ 99%) was purchased from Acros Organics (Belgium). Ethanol (EtOH, ≥ 99.8%), methanol (MeOH, ≥ 99.8%), acetonitrile (ACN, ≥ 99.9%), and glacial acetic acid (AcOH, ≥ 99.7%) were all acquired from Fisher Chemical (UK). The water used in the experiments was ultrapure water supplied by the local laboratory.

2.2. Sorbent synthesis

The synthesis of the MIS is described in Fig. 1. The first step of synthesis of the molecularly imprinted sorbent (MIS) was to join (*E*)-resveratrol with the functional monomers of 4VP and styrene in a mixture of ACN-DMF (85–15). This step allowed the assembly of (*E*)-resveratrol with the functional monomers. The second step was the addition of the crosslinker EGDMA which served as a scaffold for the pre-assembled (*E*)-resveratrol-4VP-stryene complex. The final step was the addition of the initiator AIBN (degassing with argon was performed to avoid reaction inhibition) and the reaction mixture was introduced into a UV reactor (Paralab – Portugal). This latter is equipped with four mercury vapor lamps (Philips Actinic BL TL 8 W/10 1FM/10 × 25CC) with a maximum emission at 350 nm which corresponds to the maximum absorbance of the initiator AIBN. The irradiation lasted for 24 h. A corresponding non-imprinted sorbent (NIS) was synthesized following the exact same procedure but without including (*E*)-resveratrol in the polymerization mixture. The obtained polymers were cleaned with MeOH–AcOH (9–1)

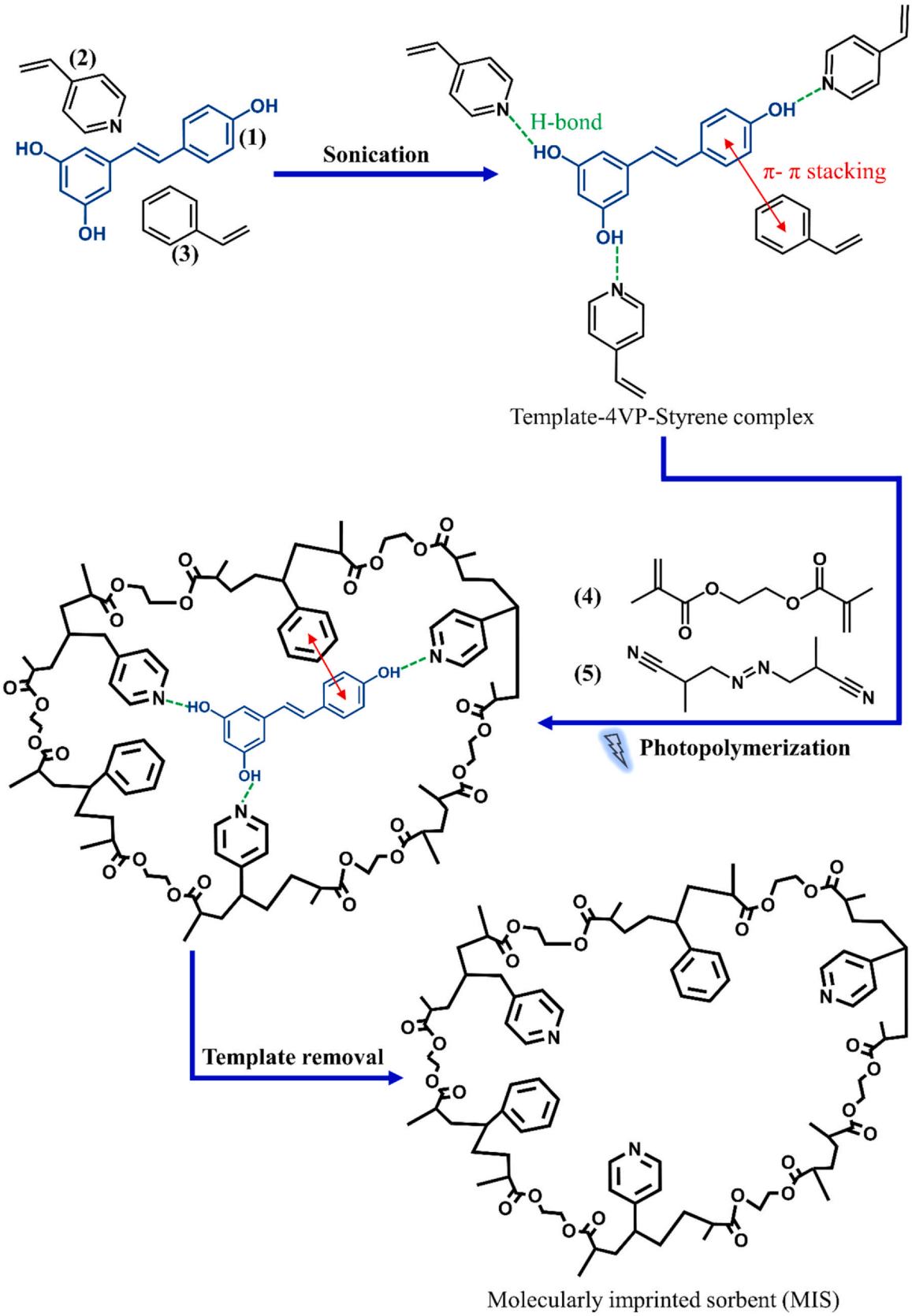

Fig. 1 – Synthesis steps of the MIS. The interaction of (*E*)-resveratrol with the functional monomers of 4VP and styrene is also depicted. (1) (*E*)-resveratrol; (2) 4VP; (3) styrene; (4) EGDMA (crosslinker); (5) AIBN (photo-initiator).

several times using a dialysis membrane (3.5 k MWCO, ThermoFisher Scientific) to remove the unreacted reagents as well as the (*E*)-resveratrol. Further steps of cleaning with MeOH and EtOH were performed to ensure the cleanliness of the sorbents.

2.3. *Material's characterization*

2.3.1. *FTIR*

The MIS and NIS were dried in a vacuum oven at 50 °C. The change in mass of the materials was followed along the

drying process until no further change was observed. After fully drying the MIS and the NIS, Fourier-transform infrared spectroscopy (FTIR) was carried out in attenuated total reflectance (ATR) mode between 4000 cm^{-1} and 450 cm^{-1}. The spectrometer used for this was a PerkinElmer Spectrum Two.

2.3.2. SEM

The microscopic morphology of the synthesized MIS and NIS was determined by scanning electron microscopy (SEM) at the International Iberian Nanotechnology Laboratory (INL), Braga (Portugal) using the FIB/SEM system HELIOS Nanolab 450 S. SEM images were obtained using an electron beam of 3 keV, a beam current of 25 pA and at field free lens mode.

2.3.3. Sorption experiments

To determine the isotherms of the materials (MIS and NIS), standard solutions of *(E)*-resveratrol with concentrations of 10, 25, 50, 100, 250 and 500 mg L^{-1} were prepared in ACN. For each concentration level, batch sorption experiments were carried out by joining a mass of 10 mg of the material (MIS or NIS) with 1 ml of the standard *(E)*-resveratrol solution. The batch mixtures were left to equilibrate for 24 h in the dark to avoid any degradations and under moderate shaking of 80 RPM. At the end of the 24 h, the liquid phase was recuperated, filtered, and analyzed by HPLC (Knauer). The chromatographic analysis was performed in gradient mode varying the mobile phase from 100% of water–ACN (9–1) to 100% water–ACN (1–9) for 45 min. The stationary phase was an Ascentis C18 (SUPELCO) column with a particle size of 5 µm and dimensions 25 cm × 4.6 mm. The flow rate of the analysis was 1 ml min^{-1} and the temperature of the column was set to 45 °C. This procedure made possible the determination of the free quantity of *(E)*-resveratrol in the liquid phase and consequently the retained quantity in the materials. The binding capacity of the materials is calculated using Eq. (1):

$$Q_e = \frac{(C_0 - C_e) \times V}{m} \quad (1)$$

Where Q_e is the equilibrium binding capacity expressed in mg g^{-1}, C_0 and C_e are the initial and the equilibrium concentrations of *(E)*-resveratrol respectively and are both expressed in mg L^{-1}. V is the volume of the standard *(E)*-resveratrol solution in ml and m is the sorbent mass in mg. The obtained isotherms were fitted to Langmuir and Freundlich models following Eqs. (2) and (3) respectively.

$$Q_e = \frac{Q_m K_L C_e}{1 + K_L C_e} \quad (2)$$

$$Q_e = K_f C_e^{1/n} \quad (3)$$

K_L (L mg^{-1}) is the ratio of the sorption and desorption rates, Q_m (mg g^{-1}) is the maximum sorption capacity of the material. K_f ($L^{1/n}$ $mg^{1-1/n}$ g^{-1}) and n are the two parameters of Freundlich isotherm.

2.4. Extraction of (E)-resveratrol form grape stems residue

The residue of grape stems was supplied by the winery of Caves Campelo (Braga – Portugal) from the fall of 2021. This residue is the result of different grape varieties as it is the approach used by this winery. The grape stems were initially ground using a laboratory mill (SM-450, MRC Lab). The obtained powder (20 g) was mixed with 200 ml of ACN and left in an ultrasound bath for 20 min. After this, the extraction mixture was left to stir for 1 h (aluminum foil was used to protect the mixture from light). The extraction mixture was then vacuum filtered to obtain the final grape stems extract. The same extraction process was replicated using EtOH-W (8–2, v/v) as a solvent, and the two extracts were analyzed by HPLC. This approach allowed us to obtain two extracts with different phenolic compositions with the ACN showing a better pre-isolation of *(E)*-resveratrol. The content of *(E)*-resveratrol in grape stems with ACN extraction was estimated to be 3700 mg/kg of dry weight, which is a value comparable to some literature references (Chernousova et al., 2022; Rayne et al., 2008; Aaviksaar et al., 2003) but scattered values on (E)-resveratrol content of vinery and winemaking residues are reported (Piñeiro et al., 2013; Sun et al., 2006; Tıraş et al., 2022). Besides the strong impact of grapes variety, geographical origin and season of collection, the extraction conditions can also lead to differences in some orders of magnitude for the resveratrol content of such kinds of biomass (dispersion also observed for other stilbenes and polyphenols in general). Here we are using a mixture of different grape varieties in order to try approaching a potential industrial process for the valorization of winemaking residues. Despite the possible high differences in the resveratrol content of the initial extracts, our goal is to demonstrate the utility of the developed MIPs for resveratrol and other stilbenes (e.g. *(E)*-ε-viniferin) enrichment.

2.5. Purification procedure

The purification procedure consists of two steps making use of the same experimental device (see Fig. 2). That device consisted of a dosing pump (Knauer – Azura P 4.1 S), a stainless-steel column (10 mm × 4.6 mm = 166,19 µL bed volume) packed with the synthesized MIS (35 mg) and a recipient for the feed solution. This set-up allowed working with a small mass of sorbent permitting to showcase the proof of concept of the MIS in the purification of *(E)*-resveratrol from grape stems extract.

2.5.1. First step of purification

The first step of purification treated the ACN grape stems extract (80 ml). This latter was fed to the column in a recycled manner for 100 min at a flow rate of 4 ml min^{-1} in such a way to pass 400 ml of the extract through the MIS (Fig. 2.a). The reason for this recycling approach is to ensure the occupation of the MIS's specific cavities by *(E)*-resveratrol (this point is further discussed in detail). Notice that prior to feeding the extract to the column, the MIS was first equilibrated with ACN. Consequently, the desorption took place using a succession of three solvents which are water (20 ml), W-EtOH (6–4) (45 ml) and MeOH-AA (9–1) (14 ml) (apparatus depicted in Fig. 2.b). The rationale for the desorbing solvents is explained in the results and discussion part. Both sorption and desorption were repeated 6 times in order to exhaust the *(E)*-resveratrol present in the extract.

Upon the completion of the 6 sorption-desorption cycles, the collected fractions of W-EtOH (6–4) were combined (total of 270 ml) and then evaporated in a rotatory evaporator at 50 °C. The residual solid was gathered and redissolved in W-EtOH (6–4) to achieve a concentration of 0.4 mg ml^{-1} constituting the first purified solution of *(E)*-resveratrol (PS1). This latter was analyzed by HPLC to determine the purity of

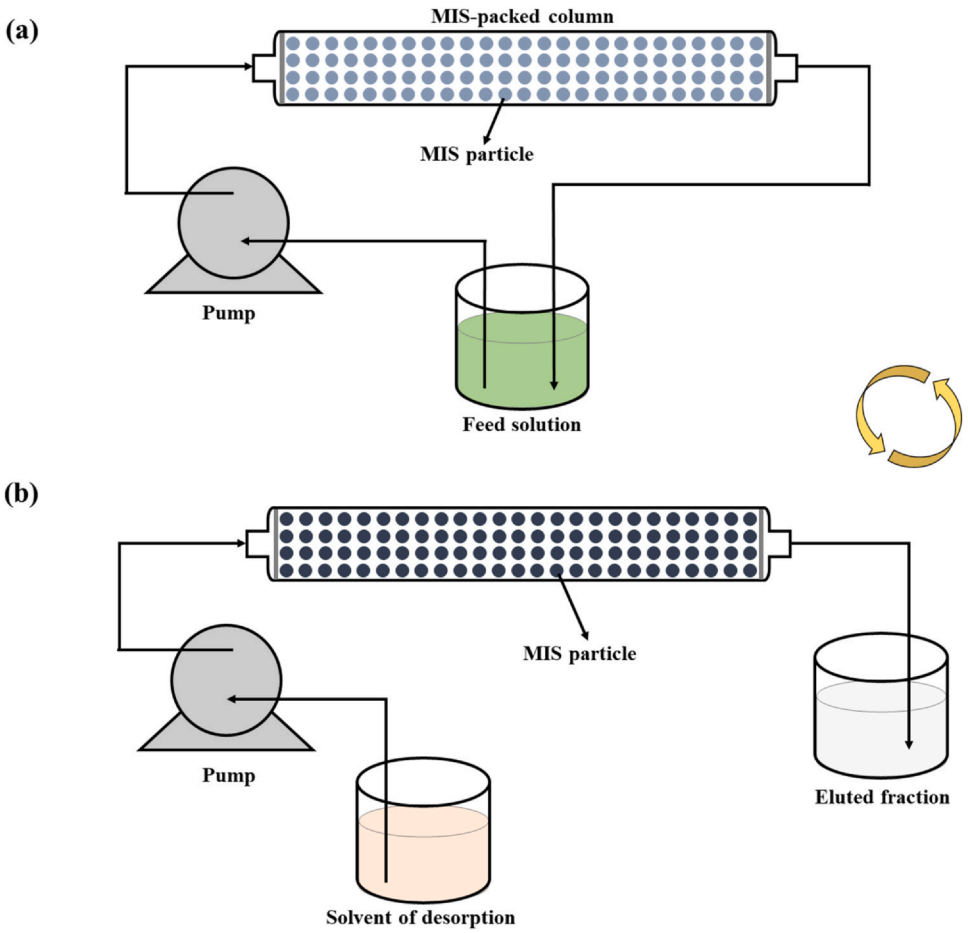

Fig. 2 – Apparatus employed to carry out the purification of *(E)*-resveratrol from grape stems extract. (a) represents the sorption phase where the feed solution is pumped into the MIS-packed column in a closed circuit to occupy the sorbent's binding sites with *(E)*-resveratrol. (b) represents the desorption phase where water, W-EtOH (6–4) or MeOH-AA (9–1) are fed into the column to elute the retained compounds. The dark blue color of the MIS particles in the desorption phase indicates the compounds retained during the sorption phase. In the first purification step, the sorption-desorption was repeated 6 times whereas for the second purification step, it was repeated 5 times.

(E)-resveratrol following Eq. (4) where C_{res} (mg L^{-1}) is the concentration of *(E)*-resveratrol in the PS1 and C_{sd} (equal to 0.4 mg ml^{-1}) is the concentration of the residual solid resulting from the evaporation of the W-EtOH (6–4) fractions.

$$P(\%) = 100\frac{C_{res}}{C_{sd}} \quad (4)$$

2.5.2. *Second step of purification*

To further enhance the purity of *(E)*-resveratrol, the MIS was equilibrated with W-EtOH (6–4) and then the PS1 was fed into the column in a recycled loop at 4 ml min^{-1} for 30 min (Fig. 2.a). The desorption was carried out by passing 15 ml of water followed by 45 ml of W-EtOH (6–4) (Fig. 2.b). This procedure was repeated 5 times to recover most of the *(E)*-resveratrol. The eluted fractions of W-EtOH (6–4) were treated in the same manner as the previous W-EtOH (6–4) fractions, leading to the second purified solution of *(E)*-resveratrol (PS2) with a concentration of residual solid equal to 0.75 mg ml^{-1}. The purity of *(E)*-resveratrol in PS2 was also determined using Eq. (1).

Both for the first and the second purification step, all the eluted fractions of water, W-EtOH (6–4) and MeOH-AA (9–1) were analyzed by HPLC to determine the amount of recovered *(E)*-resveratrol using Eq. (5). C_i and C_{feed} are the concentrations of *(E)*-resveratrol in the eluted fraction and in the feed respectively, both expressed in mg L^{-1}. V_i and V_{feed} are respectively the volumes of the eluted fraction and the feed expressed in L. For the first step of purification, n = 6 (6 cycles of sorption-desorption) and for the second step of purification, n = 5 (5 cycles of sorption-desorption).

$$R(\%) = 100\frac{\sum_i^n C_i \; V_i}{C_{feed} \; V_{feed}} \quad (5)$$

3. Results and discussion

3.1. *Sorbent synthesis*

The MIS used to carry out the purification of *(E)*-resveratrol from grape stems extract was synthesized making use of a statistical design of experiments (DoE) we have previously established (Bzainia et al., 2023). With this DoE, three parameters were varied to find the optimal polymerization recipe allowing to get a material combining high retention capability and selectivity towards *(E)*-resveratrol. For this purpose, photo-initiation allowed to trigger the precipitation polymerization. This permitted to preserve the intermolecular interactions formed between the functional monomers and *(E)*-resveratrol. Table 1 explains the three parameters considered in the DoE (2^3). The synthesized sorbents are mainly based on the functional monomer 4VP. This

Table 1 – Polymerization parameters used in the synthesis of the MIS and NIS.

Parameter	Definition	Equation
Y_M (%)	Mass fraction of the polymerizable monomers' mixture (including functional monomers and crosslinker) in the polymerization solution.	$Y_M = \frac{m_{4VP} + m_{Styrene} + m_{EGDMA}}{m_{4VP} + m_{Styrene} + m_{EGDMA} + m_{Solvent}} \times 100$
Y_{CL} (%)	Mole fraction of the crosslinker in the polymerizable monomer's mixture.	$Y_{CL} = \frac{n_{EGDMA}}{n_{4VP} + n_{Styrene} + n_{EGDMA}} \times 100$
$Y_{Res/4VP}$	Mole ratio between (*E*)-resveratrol and 4VP monomer.	$Y_{Res/4VP} = \frac{n_{resveratrol}}{n_{4VP}}$
$Y_{Res/Sty}$*	Mole ratio between (*E*)-resveratrol and styrene monomer.	$Y_{Res/Sty} = \frac{n_{resveratrol}}{n_{Sty}}$
Y_I*(%)	Mole ratio between the initiator and the polymerizable monomers.	$Y_I = \frac{n_I}{n_{4VP} + n_{Styrene} + n_{EGDMA}} \times 100$

* Y_I and $Y_{Res/Sty}$ were not considered in this experimental design, and thus fixed values of 5.2% and 1 were respectively used.

latter establishes hydrogen bonds with the hydroxyl groups of (*E*)-resveratrol conferring an anchoring site specific to (*E*)-resveratrol. The styrene monomer also adds more π- π stacking between the MIS and (*E*)-resveratrol.

The MIS used in this work has characteristic values of Y_M = 20%; Y_{CL}= 60% and $Y_{Res/4VP}$= 1/3 (in case of the NIS $Y_{Res/4VP}$ and $Y_{Res/Sty}$ are equal to zero). This specific sorbent was chosen due to its simultaneous possession of a high selectivity and sorption capacity for (*E*)-resveratrol (Bzainia et al., 2023). Moreover, from a macroscopic point of view, the particle size of the chosen MIS is adequate to perform sorption-desorption experiments without leakage of material.

3.2. *Sorbent characterization*

To confirm the polymerization of the monomers, FTIR spectroscopy was applied to the dried MIS and NIS and the obtained spectra are shown in Fig. 3. The peak at 702 cm^{-1} is characteristic of the aromatic benzene ring of the styrene monomer. Peaks at 1600 cm^{-1} (C=C pyridyl), 1418 cm^{-1} (C=N), 820 cm^{-1} and 755 cm^{-1} (both correspond to the C–H bending in the pyridine ring) (Berk et al., 2019) are all indicators of the successful polymerization of 4VP monomer and its incorporation in the polymer chains of the sorbents. Regarding the crosslinker EGDMA, its characteristic peaks appear at 1720 cm^{-1} and 1140 cm^{-1} which are assigned to the functional groups of C=O and C–O respectively (Santos et al., 2022). Clearly, FTIR spectroscopy does not reveal any structural difference between the MIS and the NIS since both sorbents consist of the same monomer units. However, the key difference between the two materials is the presence of (*E*)-resveratrol in the polymerization mixture of the MIS which in theory should significantly alter the morphology of the resulting material. Thus, to gain insight into the microscopical nature of the synthesized sorbents, scanning electron microscopy (SEM) was employed. This technique furnished valuable images for both the MIS and the NIS as shown in Fig. 4. The MIS exhibited clusters of spherical particles with a remarkably larger size than the NIS particles. This morphological discrepancy is attributed to the presence of (*E*)-resveratrol in the polymerization mixture of the MIS. This outcome is in line with previous works showing the effect of the molecular imprinting technique on the material's morphology (Gomes et al., 2020; Duan et al., 2023). In fact, during the molecular imprinting process, the template (in this case (*E*)-resveratrol) acts as a mold or a nucleation site, guiding the spatial arrangement of the monomers around it during polymerization. Thus, after the template removal, unoccupied cavities are left resulting in the overall size increase of the MIS particles compared to the NIS ones (Pardeshi and Singh, 2016). These issues were also discussed in more detail in reference (Gomes et al., 2020) concerning MIPs synthesis for the valorization of flavonoids in onion skinks residues.

3.3. *Binding experiments using the synthesized sorbents*

Although batch sorption tests were previously carried out using the exact same materials (data included in the supporting information as Fig. S1), further confirmation of those results is provided herein. The sorption of the MIS and NIS were evaluated considering six initial concentrations of (*E*)-resveratrol as depicted in Fig. 5 (the chromatograms of the

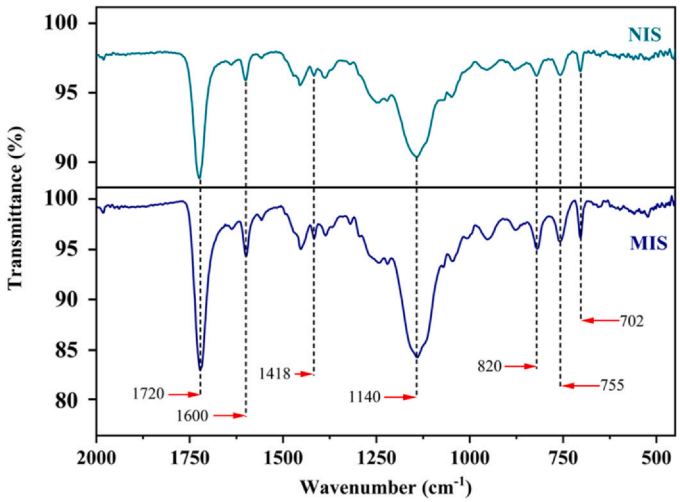

Fig. 3 – FTIR spectra of the MIS and the corresponding NIS, acquired in ATR mode.

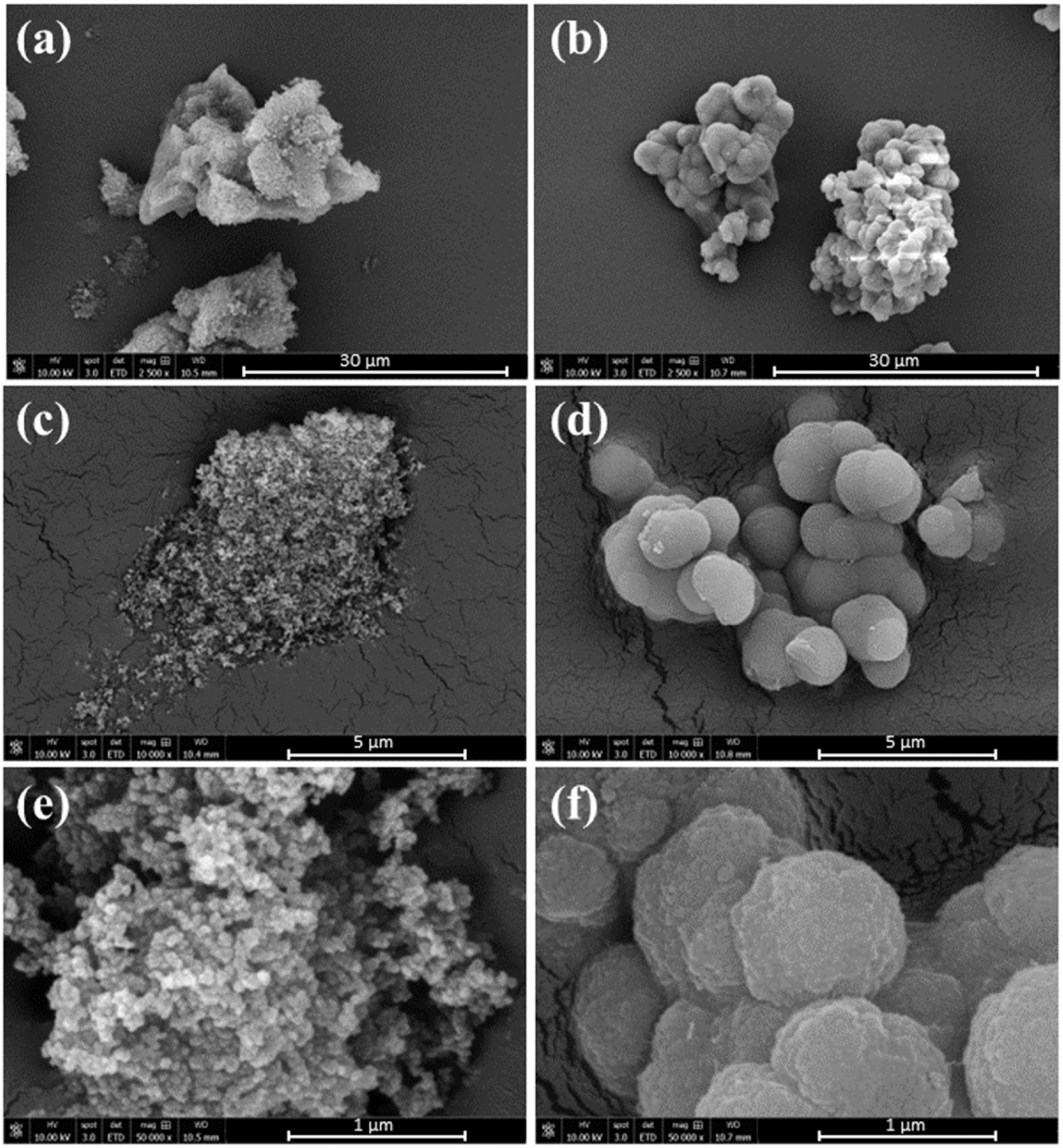

Fig. 4 – SEM images showing the morphology of the NIS (depicted in (a), (c) and (e)) and the MIS (shown in (b), (d) and (f)). Different orders of magnifications were used; (a), (b) X 2500 magnification, (c),(d) X 10,000 magnification and (e),(f) X 50,000 magnification.

liquid phases recovered in these batch tests are attached in the supporting information as Fig. S2). Regardless of the free concentration of the analyte (C_e), the binding capacity (Q_e) of the MIS was always higher than that of the NIS. This outcome is explained by the specific binding sites created in the MIS during its synthesis as proved by the SEM analysis. This does not only confer the MIS with a recognition capability for (*E*)-resveratrol, but also enhances the mass transfer through the particles of the sorbent. As a result, (*E*)-resveratrol is retained preferentially on the specific binding sites of the MIS. In contrast, the binding of (*E*)-resveratrol to the NIS particles only occurs in a non-specific manner i.e., through intermolecular interactions with the polymeric network (no specific binding sites are involved).

To elucidate the sorption of (*E*)-resveratrol on the synthesized materials, the data from our sorption experiments were fitted to both Langmuir and Freundlich isotherms models as shown in Fig. 6 and Table 2. The residual sum of squares error was the lowest when the data were fitted to the Langmuir sorption model. This good coherence between the experimental data and the Langmuir model suggests that the sorption process is homogenous and occurs at a monolayer level (Wang and Guo, 2020). Consequently, the Langmuir model provided valuable insights into the maximum sorption capacity of the materials (Q_m), revealing distinct differences between the molecularly imprinted sorbent (MIS) and the non-imprinted one (NIS). The MIS exhibited a significantly higher Q_m value of 34.95 mg g^{-1}, while the NIS had less than half of that capacity (15.74 mg g^{-1}). The higher Q_m of the MIS is attributed to the molecular imprinting process, which not only created specific binding sites for (*E*)-resveratrol but also facilitated the diffusion of the solute through the MIS particles. In addition, it can be seen that both MIS and NIS had close K_L, as indicated in Table 2, implying that the rates of sorption-desorption are comparable for both materials (Ghosal and Gupta, 2017).

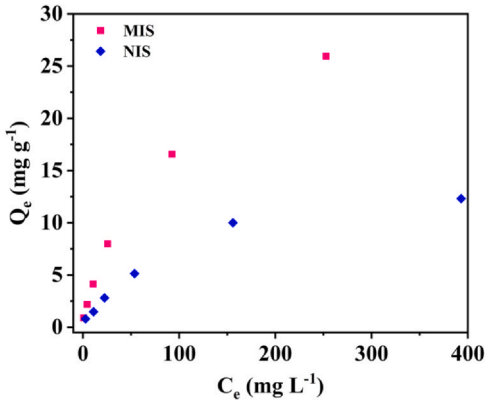

Fig. 5 – Sorption isotherms of the MIS and the NIS at 25 °C considering initial *(E)*-resveratrol concentrations of 10, 25, 50, 100, 250 and 500 mg L^{-1} in pure ACN. Q_e designates the equilibrium sorption capacity corresponding to the equilibrium concentration of *(E)*-resveratrol in the liquid phase (C_e).

3.4. *Purification procedure of (E)-resveratrol*

3.4.1. *Process design*

The objective of this work is to provide a proof of concept for purifying *(E)*-resveratrol from grape stems extract using the synthesized MIS. To achieve this, a preliminary experiment of sorption-desorption using the ACN grape stems extract was performed in order to establish the suitable conditions for the well-functioning of the purification process. The choice of ACN as the extract solvent was due to two main reasons. The first one is that the synthesized MIS is based on the 4VP monomer which depends heavily on hydrogen bonding to retain *(E)*-resveratrol (see Fig. 1). Thus, using an aprotic solvent such as ACN eliminates the interference of the solvent in this interaction. The second reason is that the ACN extract of grape stems showed a phenolic profile rich in *(E)*-resveratrol compared to the EtOH-W (8–2) solvent (both extracts are compared in Fig. S3).

The sorption of the ACN extract was performed leading to the breakthrough shown in Fig. S4. This latter shows a saturation volume of 350 ml of the ACN extract. Based on this, the saturation volume that should be used in the sorption phase should be equal or higher than 350 ml. In our case, this volume was set to be 400 ml. Nevertheless, the exact value of the saturation volume is not critical for practical applications since the concentration of *(E)*-resveratrol will vary from harvest to harvest. Moreover, even though the breakthrough shows that the MIS reached saturation, it does not imply that the binding sites of the sorbent are solely occupied by *(E)*-resveratrol.

Table 2 – Fitting parameters of the MIS and NIS by Freundlich and Langmuir models.

Sorbent	Langmuir		Freundlich	
	K_L	Q_m	n	K_f
MIS	0.013	34.95	1.87	1.36
NIS	0.010	15.74	2.07	0.73

In order to circumvent this problem, cyclic sorption of the feed solution was proposed, which allows for the re-use of the column's outlet as explained in the methodology section (see Fig. 2.a). This approach permits to forcibly fill the specific binding sites of the MIS with *(E)*-resveratrol which would result in an enhanced *(E)*-resveratrol purification. Conversely, if the sorption were to be performed in an open circuit (without re-feeding the outlet), other stilbenes with similar chemical structure to *(E)*-resveratrol would occupy those binding sites. This molecular displacement phenomenon is schematically clarified in Fig. 7 where the first image shows how the binding sites are occupied in case of a one-time feeding situation (no cycling occurring), whereas the second and third images explain how *(E)*-resveratrol displaces other compounds from the specific binding sites throughout the cyclic sorption of the feed solution. It is worth mentioning that the cycling sorption of the ACN extract adds a layer of sustainability to the purification process since the same volume of extract would be treated several times until the exhaustion of *(E)*-resveratrol.

Regarding the desorption step, the retained compounds were eluted according to their polarity. In fact, changing the polarity of the eluting solvent would result in the desorption of compounds that possess affinities to that solvent. Thus, six sequential elutions were performed using water 100% (F1), W-EtOH (6–4) (F2), W-EtOH (2–8) (F3), EtOH 100% (F4), MeOH 100% (F5) and finally MeOH-AA (9–1) (F6). The last two elutions (F5 and F6) were performed to ensure the desorption of any lingering compounds in the MIS and hence liberating the binding sites of the sorbent for the next cyclic sorption. On the other hand, the elution F1 was carried out to remove hydrophilic compounds such as phenolic acids and sugars. In fact, grapes, wine, and winemaking residues contain fair amount of sugar (Blackford et al., 2021; Ruiz-Matute et al., 2009) and thus should be eliminated to obtain fractions of *(E)*-

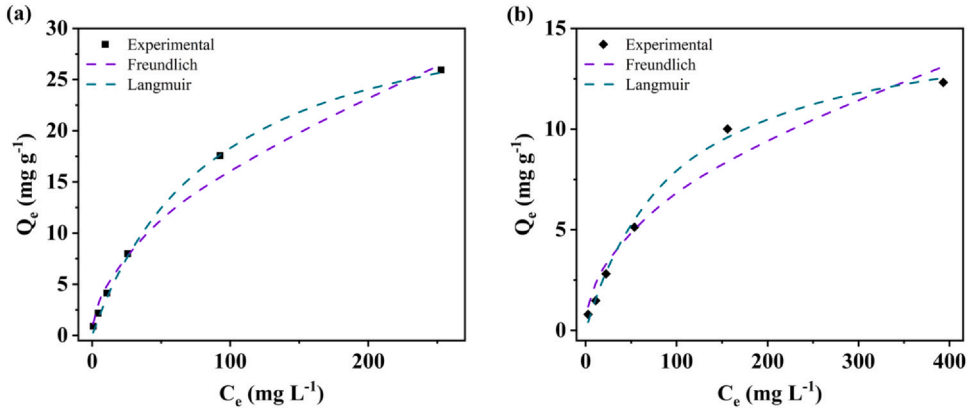

Fig. 6 – Freundlich and Langmuir models for the sorption of *(E)*-resveratrol on the (a) MIS and (b) NIS.

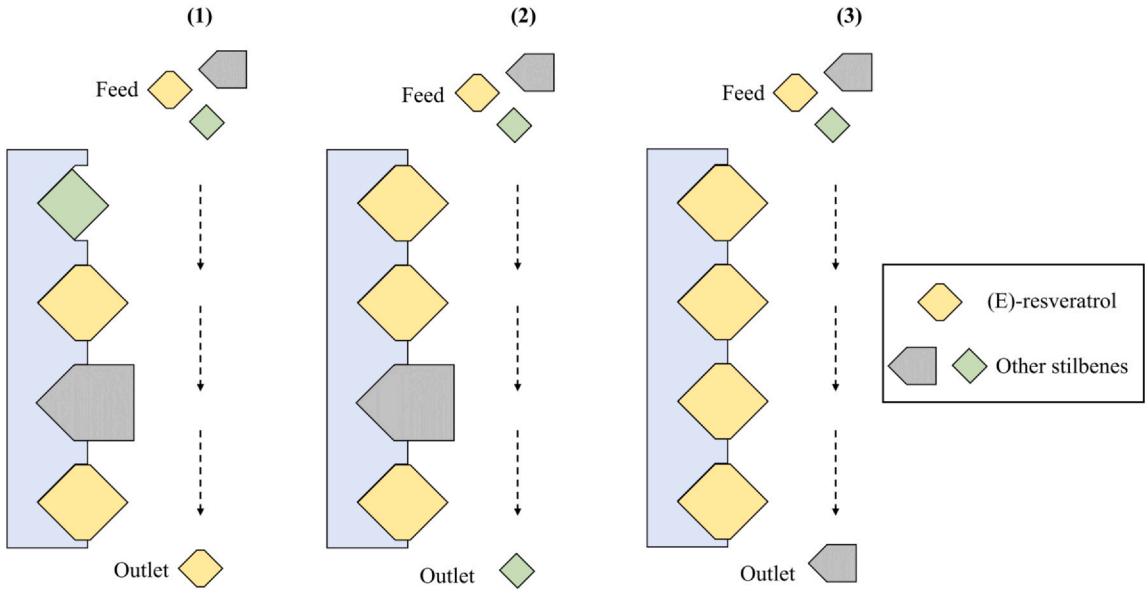

Fig. 7 – Depiction of the molecular displacement occurring in the specific binding sites of the MIS along the cyclic sorption. (1), (2) and (3) represent the different states of the MIS material throughout this sorption approach.

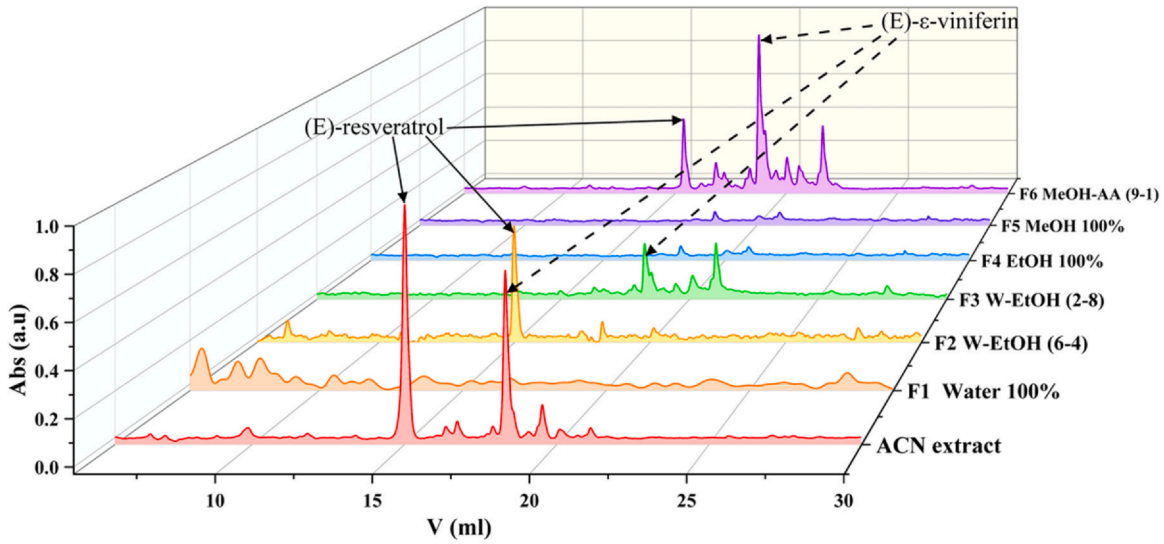

Fig. 8 – HPLC chromatograms of the eluted fractions (F1 to F6) compared to the initial ACN grape stems extract acquired (λ = 280 nm).

resveratrol with high purities. The chromatograms of the eluted fractions (F1 to F6) are shown in Fig. 8 where the isolation of *(E)*-resveratrol in the eluted fraction F2 is observed. Although *(E)*-resveratrol eluted in fraction F6 (MeOH-AA), it did so with other compounds indicating that the solvent MeOH-AA (9–1) is not suitable for the selective elution of *(E)*-resveratrol. Furthermore, fractions F3 and F4 show the elution of other compounds that potentially have a relevant bioactive activity. To verify this theory, LC-MS² analysis was carried out, which in conjunction with the UV–vis spectra allowed to identify the compound at $V_{R\ =}$ 18.5 ml as *(E)*-ε-viniferin. The data supporting these findings can be consulted in the supporting information as Fig. S5.

In fact, in some plants, the oligomers of *(E)*-resveratrol and related glucosides are biosynthesized and accumulated in order to deal with common threats (oxidative stress, defense against virus, bacteria or insects, etc.). Usually, many oxidation and condensation processes, which involve *(E)*-resveratrol as a starting unit, lead to the formation of a wide range of oligomers. The complexity of their stereochemistry increases with molecular size due to the high number of asymmetric carbons (Ito et al., 2022). As shown in Fig. 9, pterostilbene, piceatannol and *(E)*-ε-viniferin, among many others (Flamini et al., 2013; Duarte et al., 2023) are examples of *(E)*-resveratrol derivatives encountered in vines with practical interest due to their therapeutic activities (Flamini et al., 2013; Latruffe and Vervandier-Fasseur, 2018).

3.4.2. *Purification of (E)-resveratrol from grape stems extract*

Considering the findings of the preliminary sorption-desorption experiment, the purification procedure of *(E)*-resveratrol from grape stems extract was carried out following the process flowchart in Fig. 10 (part A).

Accordingly, the sorption was carried out using an ACN extract of grape stems followed by a three-step desorption commencing by water 100%, then W-EtOH (6–4) and finally

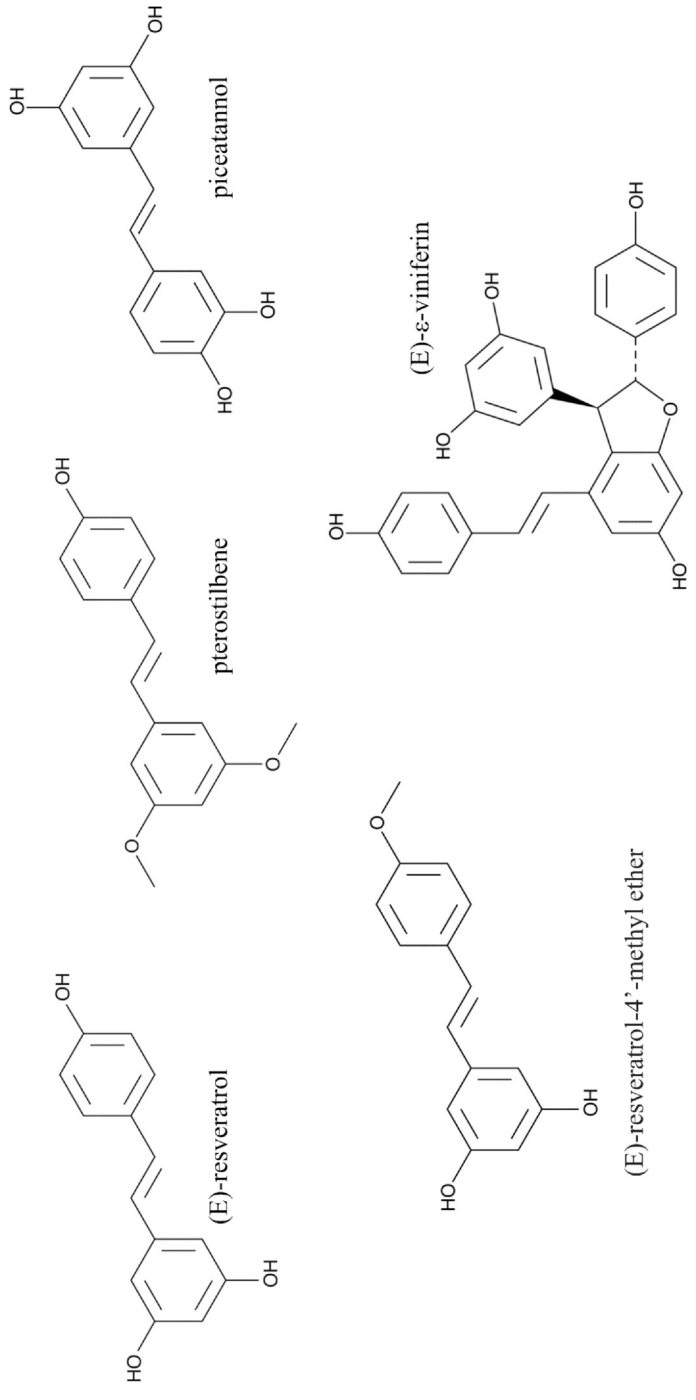

Fig. 9 – Chemical structure of (E)-resveratrol and some common derivatives found in vine (piceatannol, pterostilbene, (E)-resveratrol-4′-methyl ether and (E)-ε-viniferin). Other derivatives with complex structures can be observed in vine, grapes and related biomass (Flamini et al., 2013).

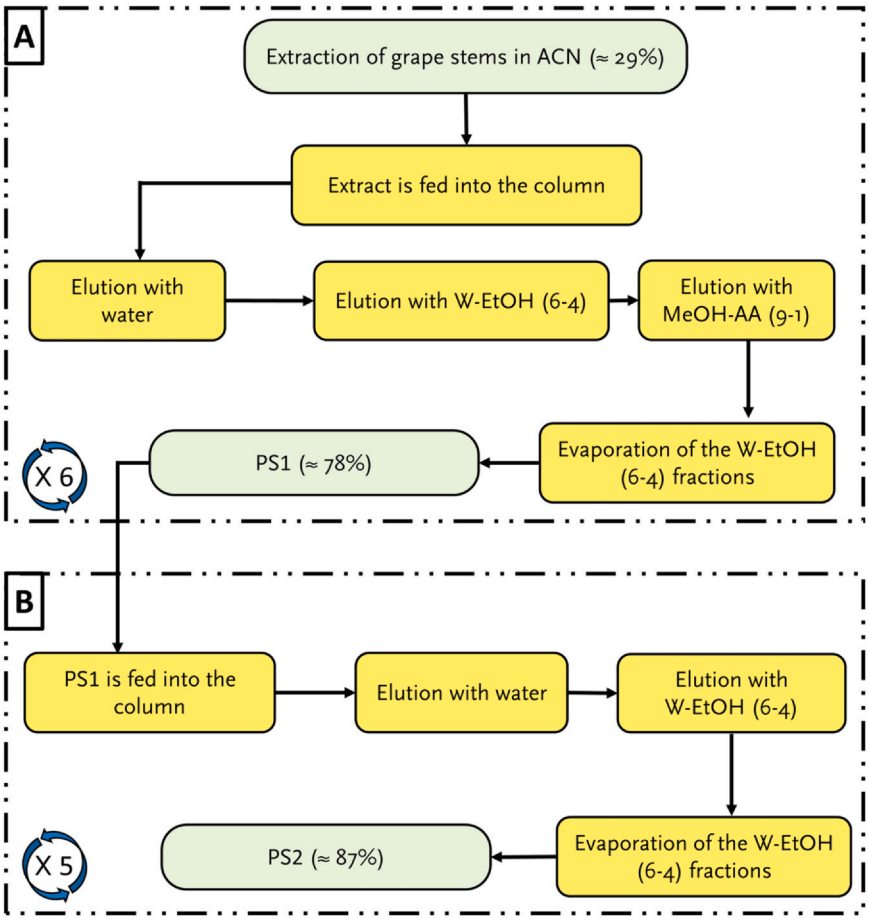

Fig. 10 – Flowchart of *(E)*-resveratrol purification process. PS1 refers to the solution of *(E)*-resveratrol at the end of the first purification step (A). PS2 refers to the solution of *(E)*-resveratrol at the end of the second purification step (B). The percentages in the green boxes are the values of *(E)*-resveratrol purities in the initial extract, PS1 and PS2.

MeOH-AA (9–1). This sorption-desorption procedure was repeated 6 times resulting in the decrease of *(E)*-resveratrol content from 30 mg to 16 mg (Fig. 11). The corresponding chromatograms of the 6 cycles are attached in the SI as Fig. S6 showing the isolation of *(E)*-resveratrol (V_R = 15.1 min) in each eluted fraction of W-EtOH (6–4). Note that from the 5th cycle to the 6th cycle, the content of *(E)*-resveratrol in the extract remained relatively unchanged (Fig. 11.b) which incited to halt the process at this stage since it is deemed sufficient to demonstrate the proof of concept of the MIS material. However, for industrial purposes, one can proceed beyond the afore-used number of cycles to exhaust all the existing *(E)*-resveratrol. The purity of *(E)*-resveratrol in the recuperated fractions of W-EtOH (6–4) was determined to be 78% which is significantly higher than the initial value of 29% in the extract. Additionally, the recovery of *(E)*-resveratrol in

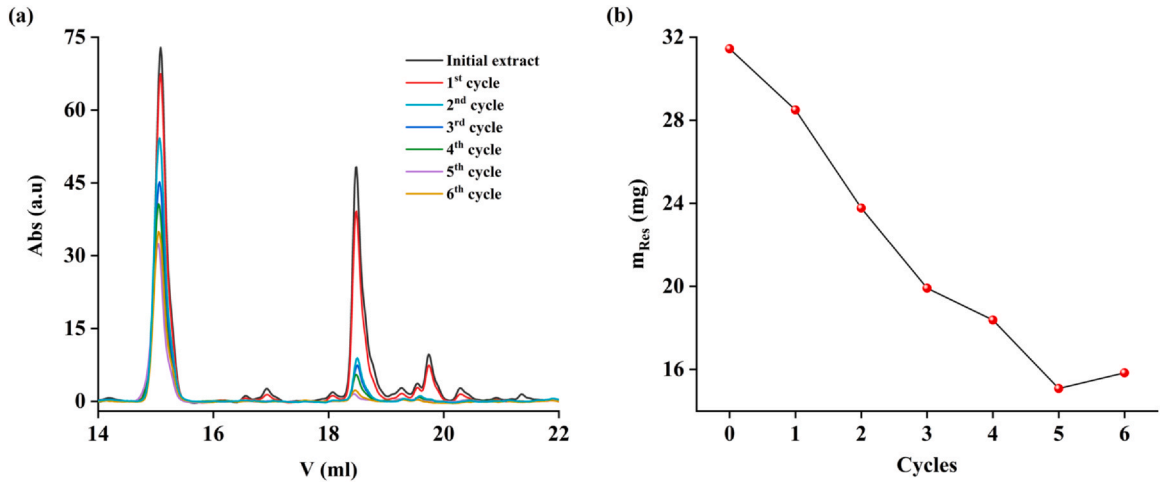

Fig. 11 – Evolution of the grape stems extract throughout the first step of purification. (a) HPLC chromatograms representing the grape stems profile after each conducted cycle (λ = 280 nm); (b) Variation of the *(E)*-resveratrol content in the grape stems extract throughout the first step of purification.

Table 3 – Processes used to valorize (*E*)-resveratrol from different matrices and their correspondent efficiencies.

Matrix	Purification procedure	Process efficiency parameters	Reference
Grape stems	Sorption-desorption based on a photo-molecularly imprinted sorbent made of 4VP.	P = 87.0% E = 3.0	This work
Muscat grape pomace	Alkaline extraction followed by foam fractionation relying on conjugates of soy protein isolate-dextran to bind (*E*)-resveratrol to the foam phase	R = 90.0% E = 6.0	(Liu et al., 2021)
Polygonum multiflormm	Static sorption of the extract using hybrid molecularly imprinted polymer based on cellulose grafted with 4-vinylpyridine chains.	P = 23.7% E = 5.6	(Cao et al., 2021)
Roots of *Polygonum multiflormm*	High speed countercurrent chromatography combined with preparative HPLC and DPPH-HPLC	P = 96.9%	(Liu et al., 2020)
Polygonum cuspidatum	Macroporous adsorption resin mixed-bed	P = 87.1% E = 1.4 R = 81.1%	(Wang et al., 2021)
Polygonum cuspidatum	Macroporous adsorption resin mixed-bed	P = 19.3% E = 5.0	(Jia et al., 2020)
Polygonum cuspidatum	pH-zone-refining counter current chromatography	P = 96.0% E = 5.5 R = 64.3%	(Yang et al., 2019)
Leaching liquor of *Polygonum cuspidatum*	Foam fractionation using ethylated β-cyclodextrin.	E = 2.8 R = 73.8%	(Liu et al., 2018)
Grape leaves	Sorption-desorption using a mesoporous carbon-packed column	P = 20.6% E = 9.8	(Sun et al., 2018)
Standard solution of (*E*)-resveratrol and naringenin.	Preferential crystallization	P ≈ 100.0% E = 1.7 R = 44.0%	(Silva et al., 2018)
Peanut sprouts	Sorption-desorption process using a commercial resin (ADS-5)	P = 23.6% E = 17.9 R = 88.3%	(Xiong et al., 2014)
Polygonum cuspidatum	Reflux extraction followed by filtration at lower pressure, hydrolyzation at pH = 1 for 8 h and at 75 °C, liquid-liquid extraction and finally alkali washing	P = 73.8%	(Wang et al., 2013)
Peanut press waste	Sorption-desorption using molecularly imprinted sorbents based on 4VP	R = 60.8% E = 60.0	(Schwarz et al., 2011b)
Polygonum cuspidatum	Macroporous resin adsorption followed by reversed phase liquid chromatography and then crystallization	P = 98.2% E = 75.5 R = 77.4%	(Zhang et al., 2009)

this 1st purification step (designed as *A* in Fig. 10) was around 34%. In fact, the non-recovered quantity of (*E*)-resveratrol is not lost since it is still in the ACN extract that eventually can be used again to retrieve more (*E*)-resveratrol.

"R" refers to recovery; "P" refers to purity and "E" signifies enrichment ratio (equal to the concentration of (*E*)-resveratrol in the final fraction divided by its concentration in the initial fraction).

Although the already obtained purity of 78% is competitive with other values encountered in the literature (Table 3), further purification can be achieved. To this end, the PS1 (78% of purity) solution was fed into the MIS-packed column in a closed circuit, and then the retained (*E*)-resveratrol was desorbed using W-EtOH (6–4) as shown in the process flowchart of Fig. 10 (part *B*). During the 2nd purification step, MeOH-AA (9–1) was not used to increase the recovery of (*E*)-resveratrol in the hydroalcoholic fractions. However, water (100%) was still used to eliminate any hydrophilic compounds. The chromatograms describing the second step of purification are shown in Fig. 12, where the W-EtOH (6–4) fractions contain (*E*)-resveratrol in an enriched manner. It can be noticed that the concentration of (*E*)-resveratrol decreased significantly in the feed solution (PS1) throughout the second purification step (Fig. 12.a) which resulted in a recovery of 70%. Moreover, the purity of (*E*)-resveratrol was determined to be 87%.

Fig. 13 recapitulates the three stages of the purification process where initially the grape stems extract contained (*E*)-resveratrol and (*E*)-ε-viniferin in the same proportions. Then, along the purification procedure, the concentration of (*E*)-resveratrol gradually increased as shown in PS1 and PS2. Additionally, the provided three-dimensional chromatograms emphasize the enrichment of (*E*)-resveratrol throughout the process.

A direct comparison of the outcome of the present work can be done with the previous work of *Cao* et al., where a material based on the same functional monomer 4VP allowed a purity of 23.7% while treating *Polygonum multiflormm* extract (Cao et al., 2021). This value is four times less than the one achieved in the present work (87%) which showcases the advantage of combining the photopolymerization with the MIT to produce tailor-made sorbents able to effectively recognize (*E*)-resveratrol in a complex mixture of compounds.

Although some works have reported high values of purities such as 96.0% (Yang et al., 2019) and 96.9% (Liu et al., 2020), they achieved such results by relying on variations of the counter current chromatography which is a more complex technique

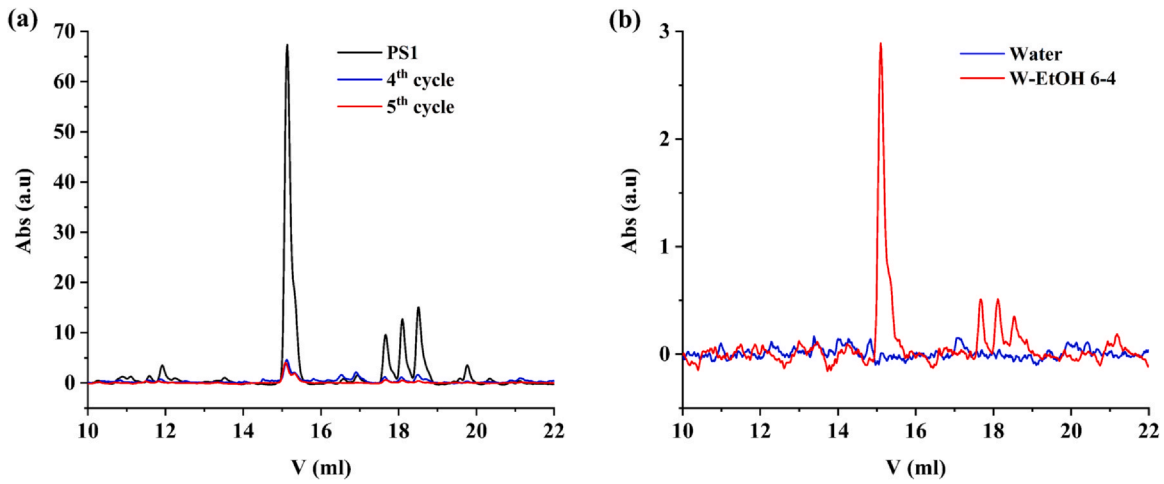

Fig. 12 – HPLC Chromatograms representing the variation of the feed solution (PS1) throughout the five sorption cycles. HPLC chromatograms of the water and W-EtOH (6–4) fractions resulting from the 2nd step of purification (λ = 280 nm).

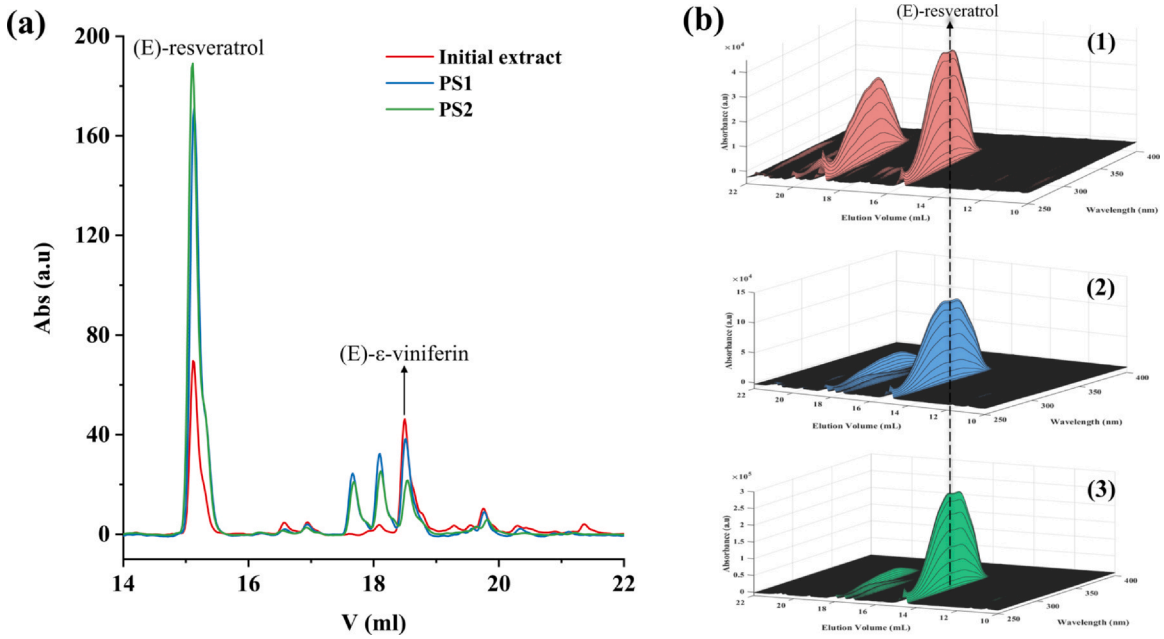

Fig. 13 – (a) HPLC chromatograms comparing the initial ACN extract with the 1st and 2nd purified solutions acquired at 280 nm. (b) 3D chromatogram of (1) ACN extract; (2) the 1st purified solution (PS1) and (3) the 2nd purified solution (PS2). The peak of *(E)*-resveratrol is around V_R = 15.1 ml whereas its derivative *(E)*-ε-viniferin is around V_R = 18.5 ml.

(compared to the sorption-desorption using the MIS) thus implying higher costs related to its potential scale-up.

Overall, the results presented above show that, in spite of an inevitable imperfect selectivity of the synthesized materials when processing complex natural extracts (e.g. MIP functional pyridyl groups interact with other phenolic groups than resveratrol), they enclose benefits as adsorbents for enrichment of resveratrol and other stilbenes (see comparison with the correspondent NIP in ref (Bzainia et al., 2023) and related discussion with commercial adsorbents in refs (Gomes et al., 2020; Bzainia et al., 2022).

The purification method here presented starts with an ACN grape stems extract due to the high resveratrol content, namely in comparison of the hydroalcoholic extract (Fig. S3). However, the direct processing of hydroalcoholic extracts with the developed MIP particles is also possible, as demonstrated above with the second step of purification (Section 2.5.2). Regarding the ACN and its potential contamination, the process developed in this work ensures its elimination up to a very low threshold due to the sequence of steps detailed in Section 2.5, that involve a huge dilution with hydroalcoholic solutions and evaporation. Considering the bed volume of the column, the volume of hydroalcoholic solutions percolated through the material and the drying process (Section 2.5) the maximum estimated concentration of acetonitrile in the final resveratrol solution is approximately 0.56 ppb. Note that acetonitrile is totally miscible with water at ambient temperature and the rotatory evaporation permits the elimination of ACN, in accordance with vapor-liquid equilibrium data (Szydłowski and Szykuła, 1999; Vapor-liquid equilibrium diagram of acetonitrile-water, 2023). According to the European Medicine Agency (EMA), and regulations for acceptable amounts for residual solvents in pharmaceuticals, acetonitrile is a class 2 solvent, meaning that its use should be limited (ICH guideline Q3C,

2019). Furthermore, EMA guideline for residual solvents, sets a limit of exposure of 410 ppm for acetonitrile (ICH guideline Q3C, 2019). This threshold is significantly higher than the maximum estimated concentration of acetonitrile in the final resveratrol solution (approximately 0.56 ppb).

4. Conclusions and perspectives

The present work demonstrates the proof of concept of molecularly imprinted sorbents as materials for the practical purification of (*E*)-resveratrol from grape stems. Precipitation polymerization initiated through UV irradiation was employed to synthesize the molecularly imprinted sorbent. This latter was characterized by FTIR spectroscopy, thus confirming the presence of the functional groups pertaining to the monomers of 4VP, styrene and the crosslinker EGDMA. Furthermore, SEM images showed that the molecular imprinting technique totally alters the morphology of the sorbent yielding larger particles for the MIS compared to the NIS. The morphology of the MIS has practical advantages in the sorption-desorption process as higher particles size results in a lower backpressure. The sorption capacities of the MIS and the NIS were determined and the correspondent isotherms were constructed. The MIS exhibited a higher sorption capacity for (*E*)-resveratrol than the NIS, which is another confirmation of the successful photo-molecular imprinting. Based on these results, the synthesized MIS was used to purify (*E*)-resveratrol from grape stems extract in a simple process of sorption-desorption. The purification process consisted of two steps during which the purity of (*E*)-resveratrol was augmented from 29% to 78% and then further to 87%. Remarkably, the purified solutions contained (*E*)-ε-viniferin which is a derivative of (*E*)-resveratrol, and its bioactivity has been demonstrated by several other studies. In spite of potential very high differences in the resveratrol content of the initial extracts (variety, geographical origin, season of collection of the biomass, extraction method), it was demonstrated the utility of the developed MIPs for resveratrol and other stilbenes (e.g. (*E*)-ε-viniferin) enrichment. The high point of this process is that the purified fractions of (E)-resveratrol were obtained in hydroalcoholic medium even though the initial solvent of the extract was ACN. This latter was intentionally used for higher stilbene extraction, namely in comparison with hydroalcoholic solvents. This outcome is important as the integration of (*E*)-resveratrol in food, cosmetic or pharmaceutical products requires its presence in a non-toxic solvent/matrix. On top of this, the pre-treatment of the grape stems extract was not needed prior to the purification process.

It is fundamental to highlight that the performance of molecularly imprinted sorbents can be influenced by factors such as temperature and pH. Therefore, careful optimization and monitoring of these parameters are necessary to ensure consistent and reliable purification results. Furthermore, while the described process eliminates the need for pre-treatment of the grape stems extract, the compatibility of this specific process with other matrices should be evaluated.

These findings substantiate the viability of scaling up the proposed process of sorption-desorption using photo-molecularly imprinted sorbents. In summary, the present work has put into evidence the role of photo-molecularly imprinted sorbents in the circular-economy through a sustainable purification process relying uniquely on sorption and desorption principles.

Declaration of Competing Interest

The authors declare that they have no known competing financial interests or personal relationships that could have appeared to influence the work reported in this paper.

Acknowledgments

The authors are thankful for the financial aid provided by "BacchusTech-Integrated Approach for the Valorization of Winemaking Residues" (POCI-01-0247-FEDER-069583), supported by the Competitiveness and Internationalization Operational Program (COMPETE 2020), under the PORTUGAL 2020 Partnership Agreement, through the European Regional Development Fund (ERDF). A. Bzainia is grateful to the national funding by the Foundation for Science and Technology (FCT, Portugal) through the PhD grant of UI/BD/153688/2022. R.D. is grateful to the Foundation for Science and Technology (FCT, Portugal) for financial support through national funds FCT/MCTES (PIDDAC) to CIMO (UIDB/00690/2020 and UIDP/00690/2020) and SusTEC (LA/P/0007/2020). M.R.C. acknowledges the support by LA/P/0045/2020 (ALiCE), UIDB/50020/2020, and UIDP/50020/2020 (LSRE-LCM), funded by national funds through FCT/MCTES (PIDDAC).

Appendix A. Supporting information

Supplementary data associated with this article can be found in the online version at doi:10.1016/j.fbp.2023.08.010.

References

A. Aaviksaar, M. Haga, T. Püssa, M. Roasto, and G. Tsoupras, Purification of resveratrol from Vine stems, *Proceedings of the Estonian Academy of Sciences. Chemistry*, vol. 52, no. 4, p. 155, 2003. doi:10.3176/chem.2003.4.02.

Acquadro, S., et al., 2020. Grapevine green pruning residues as a promising and sustainable source of bioactive phenolic compounds (Jan). Molecules, vol. 25 (3), 464. https://doi.org/10.3390/molecules25030464

Arabi, M., et al., 2021. Molecular Imprinting: green Perspectives and Strategies (Jul). Adv. Mater., vol. 33 (30), 2100543. https://doi.org/10.1002/adma.202100543

Berk, H., Balci, B., Ertan, S., Kaya, M., Cihaner, A., 2019. Functionalized polysulfide copolymers with 4-vinylpyridine via inverse vulcanization (Jun). Mater. Today Commun., vol. 19, 336–341. https://doi.org/10.1016/j.mtcomm.2019.02.014

Blackford, M., et al., 2021. A review on stems composition and their impact on wine quality (Feb). Molecules, vol. 26 (5), 1240. https://doi.org/10.3390/molecules26051240

Bzainia, A., Dias, R.C., Costa, M.R., 2022. Enrichment of quercetin from winemaking residual diatomaceous earth via a tailor-made imprinted adsorbent. Molecules, vol. 27 (19), 6406. https://doi.org/10.3390/molecules27196406

Bzainia, A., Dias, R.C.S., Costa, M.R.P.F.N., 2023. Functionalization of polymer networks to target trans-resveratrol in winemaking residues supported by statistical design of experiments (Jan). Macromol. React. Eng. 2200076. https://doi.org/10.1002/mren.202200076

Cao, J., et al., 2021. A porous cellulose-based molecular imprinted polymer for specific recognition and enrichment of resveratrol (Jan). Carbohydr. Polym., vol. 251, 117026. https://doi.org/10.1016/j.carbpol.2020.117026

Chernousova, I.V., Zaitsev, G.P., Zhilyakova, T.A., Grishin, Y.V., 2022. Biologically active agents as part of extracts of grape leaves and vine and method of their extraction (Jan). IOP Conf.

Ser. Earth Environ. Sci., vol. 954 (1), 012016. https://doi.org/10.1088/1755-1315/954/1/012016
Chopra, H., et al., 2022. Emerging trends in the delivery of resveratrol by nanostructures: applications of nanotechnology in life sciences (Mar). J. Nanomater, vol. 2022, 1–17. https://doi.org/10.1155/2022/3083728
Cormack, P.A.G., Elorza, A.Z., 2004. Molecularly imprinted polymers: synthesis and characterisation (May). J. Chromatogr. B, vol. 804 (1), 173–182. https://doi.org/10.1016/j.jchromb.2004.02.013
del, M., Contreras, M., Romero-García, J.M., López-Linares, J.C., Romero, I., Castro, E., 2022. Residues from grapevine and wine production as feedstock for a biorefinery (Jul). Food Bioprod. Process., vol. 134, 56–79. https://doi.org/10.1016/j.fbp.2022.05.005
Duan, Y., Xu, Z., Liu, Z., 2023. A multi-site recognition molecularly imprinted solid-phase microextraction fiber for selective enrichment of three cross-class environmental endocrine disruptors. J. Mater. Chem. B, vol. 11 (5), 1020–1028. https://doi.org/10.1039/D2TB02156K
Duarte, C.N., et al., 2023. Chemical characterization and bioactive properties of wine lees and diatomaceous earth towards the valorization of underexploited residues as potential cosmeceuticals (Mar). Cosmetics, vol. 10 (2), 58. https://doi.org/10.3390/cosmetics10020058
Esparza, I., Moler, J.A., Arteta, M., Jiménez-Moreno, N., Ancín-Azpilicueta, C., 2021. Phenolic composition of grape stems from different Spanish varieties and vintages (Aug). Biomolecules, vol. 11 (8), 1221. https://doi.org/10.3390/biom11081221
Fabjanowicz, M., Płotka-Wasylka, J., Namieśnik, J., 2018. Detection, identification and determination of resveratrol in wine. Problems and challenges (Jun). TrAC Trends Anal. Chem., vol. 103, 21–33. https://doi.org/10.1016/j.trac.2018.03.006
Flamini, R., Mattivi, F., Rosso, M., Arapitsas, P., Bavaresco, L., 2013. Advanced knowledge of three important classes of grape phenolics: anthocyanins, stilbenes and flavonols (Sep). Int J. Mol. Sci., vol. 14 (10), 19651–19669. https://doi.org/10.3390/ijms141019651
Ghosal, P.S., Gupta, A.K., 2017. Determination of thermodynamic parameters from Langmuir isotherm constant-revisited (Jan). J. Mol. Liq., vol. 225, 137–146. https://doi.org/10.1016/j.molliq.2016.11.058
Gomes, C.P., Franco, V., Dias, R.C.S., Costa, M.R.P.F.N., 2020. Processing of onion skin extracts with quercetin-molecularly imprinted adsorbents working at a wide range of water content (Dec). Chromatographia, vol. 83 (12), 1539–1551. https://doi.org/10.1007/s10337-020-03958-0
ICH guideline Q3C (R6) on impurities: guideline for residual solvents, European Medicines Agency (EMA), 2019, ⟨https://www.ema.europa.eu/en/documents/scientific-guideline/international-conference-harmonisation-technical-requirements-registration-pharmaceuticals-human-use_en-33.pdf⟩ (accessed Aug. 22, 2023).
Islam, F., et al., 2022. Resveratrol and neuroprotection: an insight into prospective therapeutic approaches against Alzheimer's disease from bench to bedside (Jul). Mol. Neurobiol., vol. 59 (7), 4384–4404. https://doi.org/10.1007/s12035-022-02859-7
Ito, T., Nishiguchi, M., Fukaya, M., Ryu, K., Iinuma, M., 2022. Occurrence of a resveratrol trimer diglucoside derivative with a fused heptacyclic skeleton in Shorea uliginosa (Jun). Phytochem Lett., vol. 49, 120–124. https://doi.org/10.1016/j.phytol.2022.03.013
Ji, M., Li, Q., Ji, H., Lou, H., 2014. Investigation of the distribution and season regularity of resveratrol in Vitis amurensis via HPLC–DAD–MS/MS (Jan). Food Chem., vol. 142, 61–65. https://doi.org/10.1016/j.foodchem.2013.06.131
Jia, W., Chen, Z., Zhao, Y., Ma, S., Di, D., 2020. Separation and purification of resveratrol from Polygonum cuspidatum by macroporous adsorption resin mixed-bed techology (May). Sep Sci. Technol., vol. 55 (8), 1473–1484. https://doi.org/10.1080/01496395.2019.1604755
Latruffe, N., Vervandier-Fasseur, D., 2018. Strategic syntheses of vine and wine resveratrol derivatives to explore their effects on cell functions and dysfunctions (Dec). Diseases, vol. 6 (4), 110. https://doi.org/10.3390/diseases6040110
Liu, M., Li, X., Liu, Q., Xie, S., Zhu, F., Chen, X., 2020. Preparative isolation and purification of 12 main antioxidants from the roots of Polygonum multiflorum Thunb. using high-speed countercurrent chromatography and preparative HPLC guided by 1,1′-diphenyl-2–picrylhydrazyl-HPLC (Apr). J. Sep Sci., vol. 43 (8), 1415–1422. https://doi.org/10.1002/jssc.201901287
Liu, W., et al., 2018. Foam fractionation for effective recovery of resveratrol from the leaching liquor of Polygonum cuspidatum by using partially ethylated β-cyclodextrin as collector and frother (Feb). Ind. Crops Prod., vol. 112, 420–426. https://doi.org/10.1016/j.indcrop.2017.12.035
Liu, W., He, Z., Yin, H., Yang, C., Lu, K., 2021. Maillard reaction products for strengthening the recovery of trans-resveratrol from the muscat grape pomace by alkaline extraction and foam fractionation (Feb). Sep Purif. Technol., vol. 256, 117754. https://doi.org/10.1016/j.seppur.2020.117754
Mizan, T.I., Savage, P.E., Ziff, R.M., 1996. Temperature dependence of hydrogen bonding in supercritical water (Jan). J. Phys. Chem., vol. 100 (1), 403–408. https://doi.org/10.1021/jp951561t
Pardeshi, S., Singh, S.K., 2016. Precipitation polymerization: a versatile tool for preparing molecularly imprinted polymer beads for chromatography applications. RSC Adv., vol. 6 (28), 23525–23536. https://doi.org/10.1039/C6RA02784A
Piñeiro, Z., Guerrero, R.F., Fernández-Marin, M.I., Cantos-Villar, E., Palma, M., 2013. Ultrasound-assisted extraction of stilbenoids from grape stems (Dec). J. Agric. Food Chem., vol. 61 (51), 12549–12556. https://doi.org/10.1021/jf4030129
Rayne, S., Karacabey, E., Mazza, G., 2008. Grape cane waste as a source of trans-resveratrol and Trans-Viniferin: High-value phytochemicals with medicinal and anti-phytopathogenic applications. Ind. Crops Prod., vol. 27 (3), 335–340. https://doi.org/10.1016/j.indcrop.2007.11.009
Ruiz-Matute, A.I., Sanz, M.L., Moreno-Arribas, M.V., Martínez-Castro, I., 2009. Identification of free disaccharides and other glycosides in wine (Oct). J. Chromatogr. A, vol. 1216 (43), 7296–7300. https://doi.org/10.1016/j.chroma.2009.08.086
Santos, J., et al., 2022. High-value compounds obtained from grape canes (Vitis vinifera L.) by steam pressure alkali extraction (May). Food Bioprod. Process., vol. 133, 153–167. https://doi.org/10.1016/j.fbp.2022.04.003
Schwarz, L.J., Danylec, B., Harris, S.J., Boysen, R.I., Hearn, M.T.W., 2011a. Preparation of molecularly imprinted polymers for the selective recognition of the bioactive polyphenol, (E)-resveratrol (Apr). J. Chromatogr. A, vol. 1218 (16), 2189–2195. https://doi.org/10.1016/j.chroma.2011.02.043
Schwarz, L.J., Danylec, B., Yang, Y., Harris, S.J., Boysen, R.I., Hearn, M.T.W., 2011b. Enrichment of (E)-resveratrol from peanut byproduct with molecularly imprinted polymers (Apr). J. Agric. Food Chem., vol. 59 (8), 3539–3543. https://doi.org/10.1021/jf104230f
Silva, M., Vieira, B., Ottens, M., 2018. Preferential crystallization for the purification of similar hydrophobic polyphenols (Jul). J. Chem. Technol. Biotechnol., vol. 93 (7), 1997–2010. https://doi.org/10.1002/jctb.5526
Su, L.-Y., Huang, W.-C., Kan, N.-W., Tung, T.-H., Huynh, L.B.P., Huang, S.-Y., 2023. Effects of resveratrol on muscle inflammation, energy utilisation, and exercise performance in an eccentric contraction exercise mouse model (Jan). Nutrients, vol. 15 (1), 249. https://doi.org/10.3390/nu15010249
Sun, B., Ribes, A.M., Leandro, M.C., Belchior, A.P., Spranger, M.I., 2006. Stilbenes: quantitative extraction from grape skins, contribution of grape solids to wine and variation during wine maturation. Anal. Chim. Acta, vol. 563 (1–2), 382–390. https://doi.org/10.1016/j.aca.2005.12.002
Sun, H., Lin, Q., Wei, W., Qin, G., 2018. Ultrasound-assisted extraction of resveratrol from grape leaves and its purification on mesoporous carbon (Oct). Food Sci. Biotechnol., vol. 27 (5), 1353–1359. https://doi.org/10.1007/s10068-018-0385-2

Szydłowski, J., Szykuła, M., 1999. Isotope effect on miscibility of acetonitrile and water. Fluid Phase Equilibr., vol. 154 (1), 79–87. https://doi.org/10.1016/s0378-3812(98)00438-5

Tapia-Quirós, P., et al., 2022. A green approach to phenolic compounds recovery from olive mill and winery wastes (Aug). Sci. Total Environ., vol. 835, 155552. https://doi.org/10.1016/j.scitotenv.2022.155552

Tıraş, Z.Ş., Okur, H.H., Günay, Z., Yıldırım, H.K., 2022. Different approaches to enhance resveratrol content in wine. Ciência e Técnica Vitivinícola, vol. 37 (1), 13–28. https://doi.org/10.1051/ctv/ctv20223701013

Vapor-liquid equilibrium diagram of acetonitrile-water, Dortmund Data Bank, DDBST, ⟨http://www.ddbst.com/⟩ (accessed Aug. 22, 2023).

Wang, D.-G., Liu, W.-Y., Chen, G.-T., 2013. A simple method for the isolation and purification of resveratrol from Polygonum cuspidatum (Aug). J. Pharm. Anal., vol. 3 (4), 241–247. https://doi.org/10.1016/j.jpha.2012.12.001

Wang, J., Guo, X., 2020. Adsorption isotherm models: classification, physical meaning, application and solving method (Nov). Chemosphere, vol. 258, 127279. https://doi.org/10.1016/j.chemosphere.2020.127279

Wang, R., Zhao, Y., Chen, Z., 2021. Separation and purification of resveratrol by liquid extraction assistance macroporous adsorption resin mixed-bed technology (Dec). Sep Sci. Technol., vol. 56 (18), 3106–3118. https://doi.org/10.1080/01496395.2020.1851260

Xiong, Q., Zhang, Q., Zhang, D., Shi, Y., Jiang, C., Shi, X., 2014. Preliminary separation and purification of resveratrol from extract of peanut (Arachis hypogaea) sprouts by macroporous adsorption resins (Feb). Food Chem., vol. 145, 1–7. https://doi.org/10.1016/j.foodchem.2013.07.140

Yang, L., Wang, C., Tong, S., 2019. Preparative separation of bioactive polyphenol resveratrol from Polygonum cuspidatum Sieb. et Zucc. by pH-zone-refining countercurrent chromatography (Mar). Sep Sci., vol. 2 (3), 100–107. https://doi.org/10.1002/sscp.201900007

Zhang, D., et al., 2009. Systematic purification of polydatin, resveratrol and anthraglycoside B from Polygonum cuspidatum Sieb. et Zucc (Apr). Sep Purif. Technol., vol. 66 (2), 329–339. https://doi.org/10.1016/j.seppur.2008.12.013